One photon lithography for high-quality lipid bilayer micro-patterns

M. Florencia Sánchez[1], Martín M.Dodes Traian[2], Valeria Levi[2], Dolores C. Carrer[1]**

[1]Instituto de Investigación Médica Mercedes y Martín Ferreyra (INIMEC), CONICET-Universidad Nacional de Córdoba, Friuli 2434, CC389, 5000 Córdoba, Argentina.

[2]Departamento de Química Biológica-IQUIBICEN Facultad de Ciencias Exactas, Universidad de Buenos Aires, Ciudad Universitaria, Buenos Aires, Argentina.

Key words:micro-contact printing; fluorescence correlation spectroscopy; supported lipid bilayers; cell-surface interactions; patterned surfaces.

ABSTRACT:A relevant question in cell biology with broad implications in biomedicine is how the organization and dynamics of interacting membranes modulate signalling cascades that involve cell-cell contact. The functionalization of surfaces with supported lipid bilayers containing tethered proteins is a particularly useful method to present ligands with membrane-like mobility to cells. Here, we present a method to generate micrometer-sized patches of lipid bilayers decorated with proteins. The method uses an economic micro-contact printing technique based on one-photon lithography that can be easily implementedin a commercial laser scanning microscope. We verified that both, proteins and lipids, freely diffuse within thepatterned-bilayer as assessed by z-scan fluorescence correlation spectroscopy and fluorescence recovery after

photobleaching. These resultssuggest that the supported lipid bilayerspatterns constitute an optimal system to explore processes involving directinteractions between cells. We also illustrate possible applications of this method by exploring theinteraction of cells expressing the Fas receptor and patterns of lipid bilayers containing an agonist antibody against Fas.

Introduction

Cells can respond to external stimuli through receptors located at the plasma membrane. The binding of ligands to these receptors triggers signaling cascades through the membrane and inside the cell that can elicit a biological response[1].In juxtacrinesignaling cascades, the interacting cells come into close contact and receptor-ligand recognition at the membrane interface triggers the intracellular signaling[2].This interaction is usually accompanied by a coordinated reorganization of membrane components at the cell-cell interface[3, 4, 5]. Moreover, the distribution and mobility of the agonist molecule at the membraneare intimately related to the final cellular response[3, 6, 7, 8, 9, 10, 11, 12].

To explore these signaling cascades, several efforts have been done to generate surfaces that mimic the organization and mobility of ligands in the cell membrane.In particular, supported lipid bilayers (SLBs) have been used to study processes involving cell-cell contact[12, 13, 14] since they allow incorporating tethered ligandswith mobilities that resemble those observed in a natural membrane. Also, it is possible to modulate the diffusion of both lipids and ligandsby controlling the lipid composition[15, 16, 17]. The main disadvantage of SLBs is that the whole cell membrane attached to the surface is exposed to the tethered ligand in contrast to the relatively small area that may be involved in cell-cell contact. In the particular case of the immune synapse, it has been shown that the contact area is in the sub-micron to micron scales[9, 18, 19].

Soft lithographic methods, and in particular micro-contact printing (μCP), have been used to generate surfaces attaching biomolecules with controlled sizes and geometries[20, 21, 22, 23, 24, 25].This methodology allowed, for example, exploring cellular interactions on the micron and submicron scales[6, 26] and controllingadhesion and connectivity of cells[27, 28].

To study complex processes involving cell-cell contact, the micro-contact printing and SLB technologies combined to generate confined arrays of SLBs[29, 30]alsocontaining tethered-ligands[26, 31, 32, 33, 34].Unfortunately, these methods usually require the generation of micro-contact printing masters throughexpensive lithographictechniques that may not be accessible to the worldwide scientific community. This is especially true since, in order to explore the different sizes and geometries that may be useful, the researcher often has to order the production of more than one of these masters, which are difficult to design and quite expensive.

In this work, we present a user-friendly method to generate micrometer-sized lipid bilayers patterns containingtethered ligands. This method is based on alow cost one-photon lithography technique[35]that has also the advantage of its relative simplicity in comparison to conventional electron beam- andphoto-lithography[21, 36]opening the possibility of exploring a wide variety of biological processes involving cell-cell local interactions.

Standard photolithography consistsof lighting through a mask a photosensitive resist that has been deposited on a substrate surface. As a consequence of the exposition, the resist may either become soluble or insoluble in a particular solvent. Whereas a small wavelength allows achieving higher precision, in practice many of the main micromachining technologies are basedon optical lithography, which exploits a spectral band between 300 and 450 nm[37].

In a previous work,Costantino et al[38]focusedan ultrafast laseron a film of a photopolymerizable resin deposited onto a coverslip to locally trigger the photon-induced polymerization of the resin.

The size of the polymerized region was limited by diffraction to~1 μm.To generate a master for lithography, the laser was scanned onto the resinfilm following a user-designed trajectory in which the laser is set toswitch on and off when desired. Thus, the resin is only curedin those regions illuminated by the laser and the non-polymerized resin can be simply washedaway. This technique allowed the fabrication of micrometer-sized patterned surfaces with dimensions limited by diffraction,that can be further used as molds for poly(dimethylsiloxane) (PDMS) stamps[38].Following this initial work, Kunik et al [35]showed that a similar photoreaction could be triggered using a standard one-photon excitation laser at very low power.The polymerization efficiency depended on both the laser power and the scanning speed.Moreover, they also proposed that the addition of a fluorescent dye improves this efficiency.

In this work, we used one-photon lithography to generate patches of biomembranescontainingsmall amounts of biotinylated lipidsthat allow incorporating selected proteins throughstreptavidin-biotin interactions. We assessedthemobility of membrane components using advanced fluorescence microscopy techniques and illustratethe potential applications of this new method showingthe response of cells expressing Fas receptor (FasR)interacting with lipid-patches containing an agonist antibody against FasR. Fas-mediated apoptosis is one of the most studied mechanisms of programmed cell death and has important implications in tissue homeostasis, immune responses and development[39]. Fas (also named APO-1; CD95) is a type I-membrane protein,member of the tumor necrosis factor receptor superfamily. The establishment of a cytotoxic synapse[18] through the interaction of Fas in the target cell andthe physiological membrane ligand on a T lymphocyte, triggers the receptor oligomerization followed by the formation of death inducing signaling complex (DISC) and subsequent apoptosis[40].

Materials and Methods

Micro-Contact Printing

Masters for μCP were fabricated by one-photon lithography[35]. Briefly, a drop of the UV-cure adhesive NOA86 (UV-curing adhesives, NorlandProducts, Cranbury, NY, USA) was placed on top of a microscope slide. The polymerization of the adhesive was performed either in a lithographer (TOLKET SRL, Buenos Aires, Argentina) or a confocal microscope (FV1000, Olympus, Japan) using a 405 nm diode laser (200 μW) focused with a 10X NA 0.4 microscope objective.The confocal setup we used did not have a motorized stage and thus, the size of the patterned-area was limited to the scanning area of the microscope. Therefore, we used the lithographer in those cases in which we required bigger patterned areas (~10 mm). The lithographer also hasthe advantage of allowing generating irregular, user-designed patterns that could not be easily programed with the software of the FV1000 confocal microscope. The masters including arrays of dots were fabricatedin a confocal microscope (FV1000, Olympus Tokyo Japan) illuminating each dot during1 s whereas lines were obtained scanning the sample at 1600 μm/sin the lithographer.Samples were rinsed with acetone and isopropyl alcohol to remove residual adhesive. PDMS stamps were obtained by pouring Sylgard 184 prepolymer (Dow Corning, Midland, MI, USA) with cross-linker in a 10:1 ratio, degassing in a vacuum, and curing 4 hs at 60°C. Then, the elastomer was peeled off the master glass coverslip. The stamp was inked with 1 mg/ml bovine serum albumin (BSA)(Sigma Aldrich St. Louis, MO, USA) and pressedagainst a coverslip for 10 min to transfer the protein onto the glass. Finally, a home-made chamber was glued onto the coverslip.

Generation of supported lipid bilayers

SLBswere prepared by the vesicle fusion method[16]. Briefly, dioleoylphosphatidylcholine(DOPC):cholesterol (Chol) (Avanti Polar Lipids, Alabaster, AL, USA)were dissolved in chloroform:methanol 2:1 at a proportion DOPC:Chol75:25mol:mol. This sample was supplementedwith 0.25 mol% of 1,2-dipalmitoyl-sn-glycero-3-phosphoethanolamine-N-(biotinyl) (PE-B), 2 mol% of phosphatidylserineand either the fluorescent lipid analogue 3,3′-dilinoleyloxacarbocyanine perchlorate (DiO-C18) or1,1′-dihexadecyl-3,3,3′,3′-tetramethylindocarbocyanine perchlorate(DiI-C16) (Molecular Probes, Eugene, OR, USA)when specifically stated. The concentration of fluorescent lipid was 0.1 and 0.01 mol% for imaging and for FCS experiments, respectively. Lipids were sequentially dried under a nitrogen flux and under vacuum for 3 h and rehydrated to a final concentration of 1mM in phosphate buffered saline (PBS). Then, lipid samples wereresuspended by vortexingand sonication to obtain small unilamellar vesicles which were further supplemented with 0.01 M $CaCl_2$. The lipid suspension was applied onto the printed coverslip and incubated for 1 minute.

Binding of proteins to SLBs

SLBs were incubated for 30 min with 1 µg/ml streptavidin(Molecular Probes, Eugene, OR, USA) for confocal imaging. Samples werewashed thoroughly to remove unbound streptavidin and sequentially incubated for 30 min with 1 µg/ml biotinylated primary anti-Fas antibody(AbCam, Cambridge, MA,) and 1 µg/ml secondary antibody (Anti-Mouse IgG-AlexaFluor 546, Molecular Probes, Eugene, OR, USA) with washing steps after each incubation.

For z-scan fluorescence correlation spectroscopy (z-scan FCS) measurements,SLBs were incubated for 30 min with 0.01 µg/ml mM streptavidin-AlexaFluor 555 (Molecular Probes, Eugene, OR, USA) and 0.01 µg/ml of biotinylatedanti-Fas antibody (AbCam, Cambridge, MA)when explicitly stated.

Confocal imaging

Confocal imaging was performed in a laser scanning confocal microscope Olympus FV300(Olympus, Japan) using a 60X NA 1.3 oil-immersion objective. DiO-C18 and AlexaFluor 555 probes were excited using the488 nm Ar laser lineand a 543 nm He-Ne laser, respectively. The lasers power at the sample was set to 13 μW. Fluorescence was collected at 510-540 nm(DiO-C18) and 565-610 nm (Alexa-Fluor 555).

Fluorescence recovery after photobleaching (FRAP)

FRAP measurements[41]were carried outina FV1000confocal microscope (Olympus, Japan)using a 60X NA 1.4 oil-immersion objective. A circular region(radius =3μm) was photobleachedby repetitively scanning the laser (20μW) for 20 s. The laser power was then decreased to 6μW and fluorescence recovery was followed by repetitively imaging a ROI containing the photobleached region at 0.1 frames/s. The intensity at the bleached region was corrected for photobleaching during imaging and used to construct the recovery curve as described previously[42, 43]. The following, empirical equation was fitted to the recovery curve:

$$FRAP(t) = \sum_{i=1}^{n} A_i \left(1 - e^{-t/\tau_i}\right) \qquad (1)$$

whereA_i is the amplitude of each component, $t$represents time after photobleaching and $\tau_i$the time constant of each component. The mobile fraction (Mf) was calculated as:

$$\mathrm{Mf} = \frac{F_\infty - F_0}{F_i - F_0} (2)$$

whereF_i is the intensity prior to the photobleaching step, F_0 the fluorescence intensity immediately after photobleaching and F_∞ is the intensity at the end of the FRAP experiment.

Mf values reported in this work are the mean ± standard error obtained from 6 independent measurements.

Z-scanFluorescence correlation spectroscopy

FCS measurements were performed in a FV1000 confocal microscope with the detector set in photon counting mode using a 60X NA 1.4 oil-immersion objective. The laser power was set to 9.7 μW and 3.5 μW for 488 and 543 laser lines, respectively.Datawere collected at a frequency of 100000 Hzduring 18 s.The normalized autocorrelation function was calculated as:

$$G(\tau) = \frac{\langle I(t) \cdot I(t+\tau) \rangle}{\langle I(t) \rangle^2} \qquad (3)$$

where I(t) is the fluorescence intensity and τ is a lag time.

The diffusion coefficients (D) of both lipids and membrane-bound proteins were determined by the z-scan method[44, 45]. Briefly, we measured fluorescence autocorrelation function at different positions along the optical axis (z axis) with a step-size of 300 nm. We fitted the experimental autocorrelation data measured at each $z_i$position with the following expression[46]:

$$G_i(\tau) = \frac{1}{N_i} \frac{1}{\left(1 + \frac{\tau}{\tau_{D,i,}}\right)} \qquad (4)$$

where$\tau_{Di}$and N_i represent the diffusion time and mean number of fluorescent molecules in the observation volume measured at z_i, respectively.

The diffusion coefficient was obtained by fitting the experimental data with the following expressions[45]:

$$\tau_D(\Delta Z) = \frac{\omega_0^2}{4D} \cdot \left(1 + \frac{\lambda^2 \Delta Z^2}{\pi^2 \omega_0^2}\right) \qquad N(\Delta Z) = N_0 \cdot \left(1 + \frac{\lambda^2 \Delta Z^2}{\pi^2 \omega_0^2}\right) \quad (5)$$

where λ is the wavelength of the excitation light, $\Delta Z = z_i - z_o$, z_o is the membrane position, $\omega_0$is the beam waist at the focus and N_o is themean number of fluorescent moleculeswhen $\Delta Z = 0$.

D values reported in this work are the mean ± standard errorobtained from at least 10 independent measurements.

Cell treatments

Subconfluent 293 HEK cells were transiently transfected with FasR-eGFP plasmid (gently provided by Petra Schwille, Max Planck Institute of Biochemistry, Martinsried, Germany). After 24 hrs, cells were trypsinized, pelleted by centrifugation,resuspended in fresh medium and placed ontothe patterned-supported bilayers. Cells were incubated at 37°C for 3 to 6 hours in DMEM (Life Technologies, Carlsbad, CA, USA)with 10% fetal bovine serum (Life Technologies, Carlsbad, CA, USA).

Results and Discussion

Micro-patterned surfaces generated by one photon lithography

We followed the one-photon lithography procedure describedin Materials and Methods to generate masters with dots sizing 2 to 20 μm or lines with widths of 10 μm. Briefly, a drop of the adhesive NOA86 was placed over a standard microscope slide and the sample was scanned with a 405 nm laser as described in Materials and Methodsto trigger thepolymerization of the adhesivein the selected areas.PDMS stamps obtained from these masters were incubatedwitha BSA solution and brought into contact with a clean coverslip to transfer the protein and passivate the surface. After this procedure, unilamellar vesicles of DOPC:Chol (75:25) mol:mol, containing small amounts of the fluorescent probe DiO-C18 were added to the treatedcoverslips (Figure 1A).

Figure 1Bshows representativeconfocal images of a small region of the lipid bilayer patterns with different designs;the patterned area covered 1 cm^2 and the design was repeated

homogeneously.The SLB selectively assembled onto regions of clean glass avoiding the passivated regions of the surface. The fluorescence intensity at the lipid bilayer spots was 2 orders of magnitude higher than that of the background confirming the efficiency of the passivation process. We analyzed the size and intensity distributions of patterned bilayers and observed that the size of the features were reproducible with a 5-8 % precision whereas their intensity varied in 21-25 % (see also Figure S1).

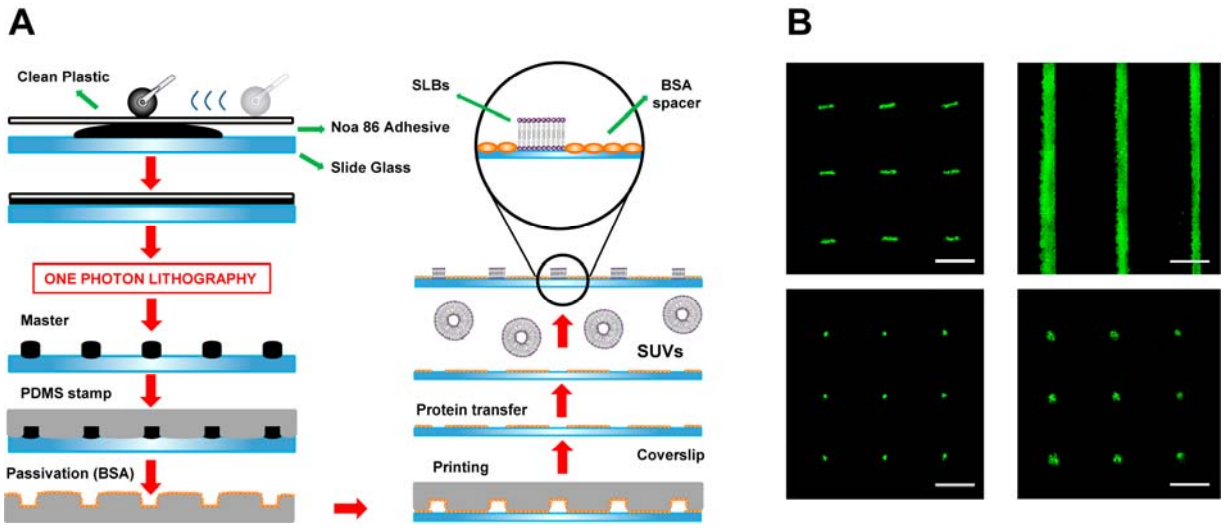

Figure 1.Generation of micrometer-sized patterns of supported lipid bilayers (A) Schematic diagram of the micro-contact printingprocedure used to generate SLB patterns.Adrop of a UV-cure adhesive is placed on top of a microscope slide and homogeneously distributed.Then, the laser is scanned to trigger the photopolymerization of the adhesive in those regions selected by the user. After removing the unpolymerized resin by washing, PDMS is cured onto this master for 4 hs at 60°C and then peeled off to generate the stamp. This stamp is passivated withbovine serum albumin for 15 min. and appliedonto a coverslip to transferthe protein.Finally, small unillamelar vesicles are added onto the coverslip to form SLB patterns in those regions free of protein.The black circle shows a zoom-in scheme of the patterned bilayer(B)Confocal images of

patterned SLB ofDOPC:Chol (75:25mol:mol), DiO-C18 0,1mol%. The size and shape of the design was controlled from the confocal microscope software as indicated in the text. Scale bar, 20 µm.

In order to assaywhether this methodologyallows generating a patterned surface functionalized with ligands of biological interest we used abiotin-streptavidin-biotin "sandwich" conjugation protocol[47] depicted in Figure 2A to include in the patches an anti-Fas antibody known to act as a model ligand for the death receptor Fas[48, 49]. With this aim, we generated patterned SLB that included a small amount of a biotinylated lipid and sequentially added streptavidin and thebiotinylatedanti-Fas antibody as described in Materials and Methods. Toverify that the antibody was efficiently incorporated in the SLB, we used anAlexa 546-labeled secondary antibody and simultaneouslyobserved the fluorescence of the DiO-C18 and Alexa 546 probes as described in Materials and Methods. Figure 2B shows a clear colocalizationof these probes. Control experiments in which we did not include either the biotynilated lipid, streptavidin or the primary antibody did not show significant fluorescence in the red channel showing that these results were notconsequence ofunspecific binding of the secondary antibody(Figure S2).

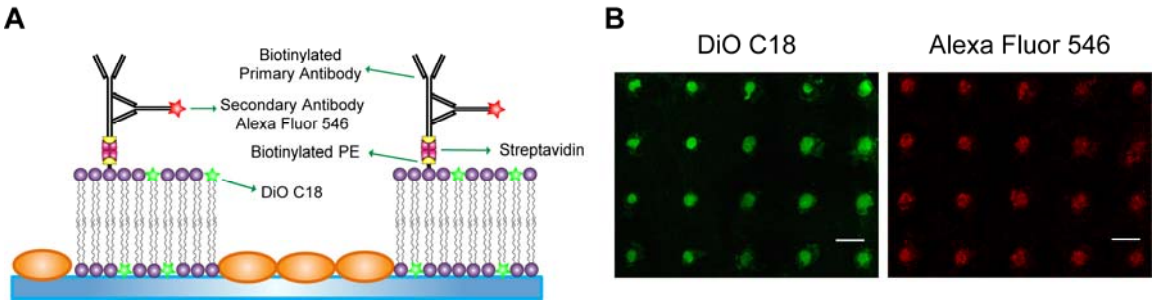

Figure 2.Generation of patterned SLBs containing anchored proteins (A) Schematic representation of the incorporation of agonist antibodies tethered to the SLB through a biotin-streptavidin linker. The fluorescent, secondary antibody was included in the membrane to assess the incorporation of the primary antibody (B) Confocal images of the patterned SLBs obtained simultaneously for DiO-C18 and AlexaFluor 546 probes as described in Materials and Methods. Scale bar, 20 μm.

Mobility of biomolecules within SLB patterns

A robust method for SLB patterning requires that molecules within patterns presentlateral motilities similar to those expected for a fluid membrane. Thus, we explored the fluidity of SLB-patches using two complementaryfluorescence microscopy approaches.

We first performed FRAP experiments to determine the mobile fraction of the fluorescent membrane probe DiO-C18 within SLBs micrometer-sized dots(Figure 3). Performing FRAP experiments in such a confined area complicates the calculation of the immobile fraction since the recovered intensity also depends on the available pool of remaining fluorescent molecules. Thus, we constructed a pattern of connected dots that guarantees a continuous supply of fluorescent molecules into the bleached area. We should point out that it is not possible to quantitatively recover the diffusion coefficients of the fluorescent molecules using this experimental approach since the kinetics of the recovery will be limited by the connection between dots. Thus, it is not possible to analyze the data with theoretical models that consider a continuous and homogeneous biomembrane[42, 43].

The mobile fraction determined from these FRAP experiments was87± 4 %indicating thatmost molecules freely diffuse within the bilayer.

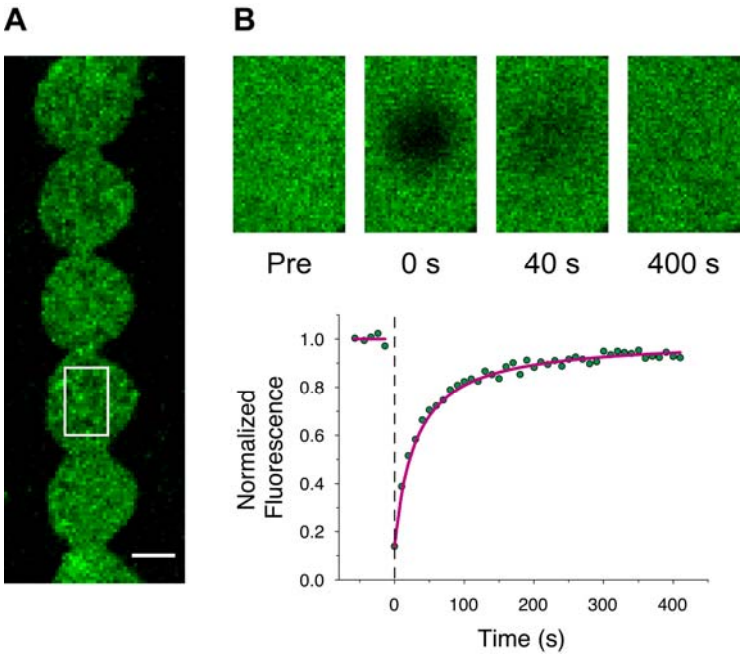

Figure 3.Assessing the mobility of biomolecules in patterned SLBs by FRAP experiments (A) Confocal image of patterned SLB containing the probe DiO-C18. Fluorescence in a 3 μm diametercircular spot was bleached as described in Materials and Methods and the laser power was diminished to observe the recovery of fluorescence acquiring images at 0.1 frames/s (B) Representative images during the recovery process. The recovery curve was obtained as described in the text and fitted with a bi-exponential function (continuous line). The mobile fraction was calculated as mentioned in Materials and Methods. Scale bar, 5μm.

Wefurther explored the dynamics of molecules at the centre of 10 μm SLB dots using z-scan fluorescence correlation spectroscopy.This calibration free- method is used to explore the mobility of biomolecules included in membranes since itovercomes the need for exact vertical positioning of the confocal volume FCSmeasurements in planar lipid systems[46, 50, 51].

We used this method to determine the diffusion coefficientsof the fluorescent probe DiO-C18 and of proteins tethered to the membraneat the center of SLB dots(Figure 4).

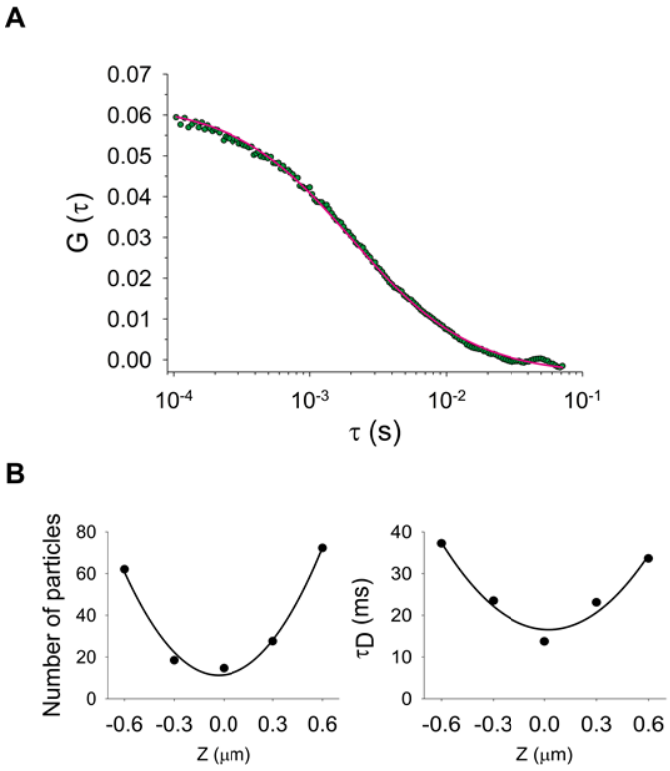

Figure 4.Measuring the dynamics of biomolecules in SLB patches by z-scan FCS. (A) Representative experimental autocorrelation curve obtained at a SLB-dot for DiO-C18 fluorescent probe with Eq. 4 fitted to the data (continuous pink line). (B) Themean number of fluorescent particles in the observation volume and their residence time were obtained by fitting Eq.4 to the experimental autocorrelationcurve at different Z positions and then plotting them as a function of ΔZ. The continuous lines show the fitting of Eq.5($\chi^2 = 10^{-5}$).

The diffusion coefficients obtained forthe studied molecules in the patterned SLB were1.58 ± 0.39 $\mu m^2/s$ (DiO-C18); 1.40 ± 0.41 $\mu m^2/s$ (streptavidin-AlexaFluor 555) and 1.27 ± 0.23 $\mu m^2/s$ (streptavidin-Alexa Fluor 555-anti-Fas). These values were not significantly different from

thosemeasured in homogeneous bilayers of the same compositions (~ 1.2 μm^2/sec)[45, 52] indicating that the confinement of molecules within the patterned-bilayers did not affect their mobility. In addition, the diffusioncoefficients of the tetheredproteins were not significantly different from that measured for the membraneprobe suggesting that the membrane viscosity limits the mobility of the proteins in the patterned SLB as was verified in both giant unilamellar vesicles and SLBs[45, 53, 54].These results show that the fluidicbehaviour of the patterned-SLB is similar to those obtained for extended biomembranesbut they also provide themicrometer-scale confinement required for controlled localization of stimuli.

Interactions of cells expressing Fas receptors and SLBs patches with tethered FasR agonist.

To test the biocompatibility and potential uses of the patterned SLBs, we prepared bilayers spotsor lines sizing 2 to 6μm containing the primary agonist antibody previously mentioned that acts as a model ligand for the death receptor Fas[48, 49].

Then, we added HEK cells transfected with FasR-eGFP in the observation chamber and let them attachonto the surface.The morphology of the cells attached to the patterned SLBs was similar to that observed for cells plated onto clean coverslips (Figure S3). After 3-6 hs, we observed that Fas receptor redistributes within the membrane presenting higher concentrations in specific regions thatcolocalized with the Fas agonist pattern. These results provide evidence of the specific interaction between FasR and its agonistat the specific lipid bilayer patches(Figure 5A). In contrast, control SLBs in which the addition of the primary antibody was omitted did not induce the formation ofFasR clusters.

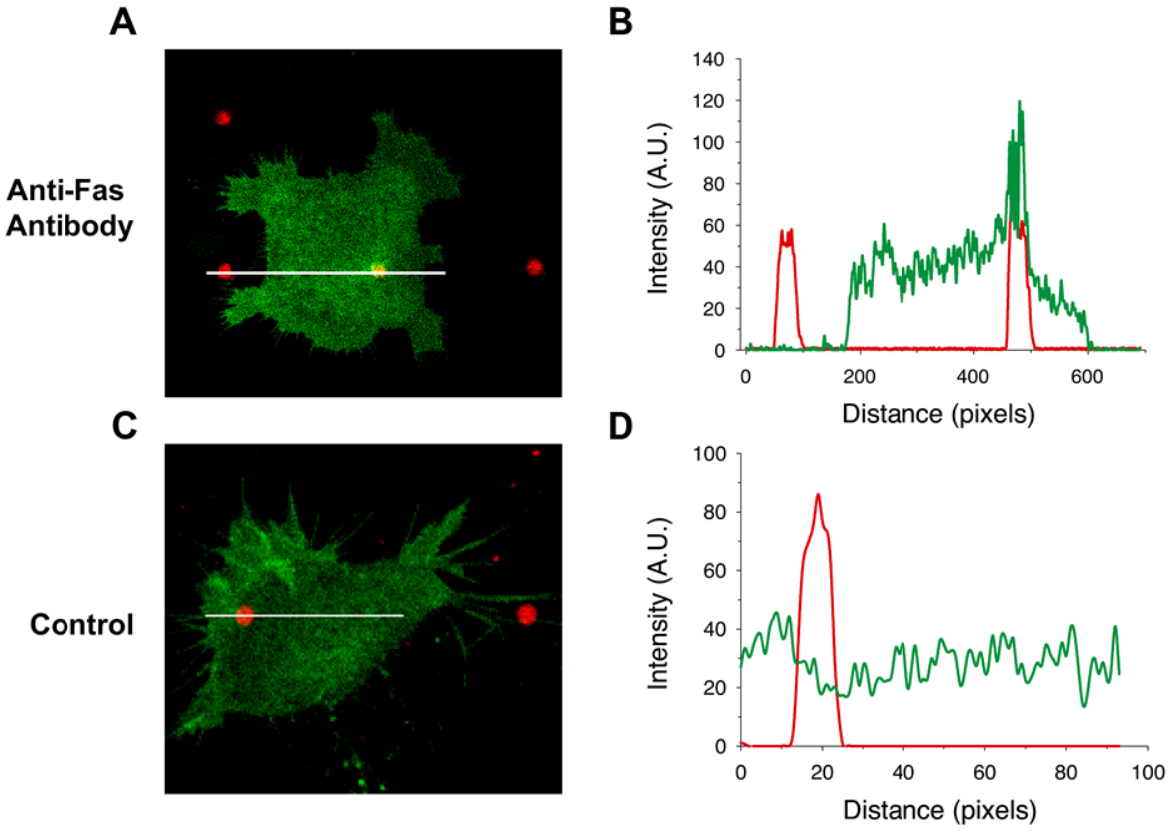

Figure 5.Confocal images of HEK cells expressing FasR-eGFPand plated onto SLBs patches containing anti-Fas and DiI-C16. The microscope was set to collect simultaneously the fluorescence of FasR-eGFP (green) and the membrane probe (red). (A, C) Overlay between the images obtained for representative cells in the green and red channels.(B, D) Intensity profiles observed along selected lines (white) for the red and green channels in treated (A,B) and control (C, D) cells. Scale bar, 10 µm.

Conclusions

The immune synapsehas emerged as a compelling model of cell-cell communication. The interface between cells involves the dynamical interactions between numerous receptor-ligand

pairs among other signalling molecules[55]in a micrometer and submicrometer region of the cell membranes[9, 18]. We now know that this synapse is a key element to coordinate the final cellular response in relevant processes such as development, homeostasis and cellrepair[56, 57, 58].

In recent years, several efforts have been made to generate synthetic micrometer-sized surfaces that mimic the natural antigen-presenting region of a cellmembrane[21, 59, 60]. Furthermore, immunotherapeutic strategies that include the use of such artificial antigen-presenting membraneare nowbeing explored as treatments for clearing pathogens in a wide range of diseases, including HIV infection, cancer and autoimmunity[2, 61, 62, 63].

During the past decade, micro- and nano-scale patterning techniques have been used to generate surfaces containing immobilized ligands[64, 65]. Despite these approaches failing to reproduce a very important membrane property, i.e. the lateral diffusion of its components, they were very useful to show that the confinement of the ligand to a surface determines adifferent response in the interacting cell. However, several evidences also indicate that cell response is intimately related to the ligand mobility[3, 12, 66]. For example, Ketchum et al. [12] has explored the response of B cells to antigens adsorbed on glass or tethered to planar lipid bilayer surfaces and found that both antigens were able to form clusters of receptors however, B cells interacting with mobile ligand displayed greater signaling than those interacting with immobile antigens. In the same direction, Hsu et al.[67] showed that the mobility of ligands anchored to supported lipid bilayers modulates the immunological synapse formation and T cells activation. In the last year, micropatterningtechnologysuch as photo-[36], and electron beam-lithography[68]followed by micro-contact printing or polymer lift-off[21]have offered broad possibilities in the field since they allowed engineering a bilayer of controlled composition and mobility containing user-selectedanchored biomolecules.Unfortunately, these methods normally include time-consuming

protocols and require expensive reagents in addition to special lithography facilities limiting the potential applications

In this work, we presented asimple and low-cost approachthatallows the generation of functionalized surfaces of controlled composition and fluidityusing only a rudimentary laser-scanning microscope.The method constitutes an easy-to-follow protocol to construct a large and reproducible array of micrometer-sized lipid bilayer motifs of user-defined size and geometry.

In addition,the same setup (i.e. a confocal microscope) could be used for generating the master and performing the microscopy observations of the sample speeding up experiments. New masters with user-designed patterns can be easily generated in a matter of a dayin contrast to the long procedure involving several steps required in classical lithography techniques such as plasma oxidation or reactive ion etch, involved in the modification and cleaning of silicon and PDMS surfaces[31, 33, 52]. Also, it is not necessary to silanize the masters[52] since in our case they are prepared directly onto the glass slide.

These advantages are particularly important for research groups out of central countries where access to clean room facilities is difficult and lithography masters normally are brought from abroad introducing a delay in the natural evolution of the research lines.

SLBs patches obtained with this methodologyhave fluid properties comparable to those of biological membranes. We also showed that it is possible to generate SLBs patterns presentingfunctional ligands. Moreover, cells could attached to these patterns, grow normally and their membrane reorganized in response to the SLB-tethered ligands.

We believe that the simplicity of this new patterning method makes it extremely versatile and a promising tool to explore cell signaling processes involving cell-cell interactions. In addition, SLB patterns decorated with proteins of interest tethered to the bilayer through the biotin-

streptavidin linker could be incorporated in biosensor devices for diagnostics and drug screening purposes[69, 70, 71].

*Corresponding authors: dolorescarrer@immf.uncor.edu, vlevi12@gmail.com

Funding Sources:This work was financially supported by SeCyT-UNC, ANPCyT Young Researchers Grant (PICT-2008-0171), ANPCyT (PICT 2008-1104), ANPCyTPRH Grant (PICT 76) andAlexander von Humboldt Foundation Alumni Grant for Equipment.

Acknowledgments: The authors wish to thank Dr. Dario Kunik for guiding us in one-photon lithography technique, help in the installation of the Tolket lithographer and for valuable and helpful discussions. Thanks are due also to Dr. Thomas Weidemann who gently provided us with the FasR-eGFP plasmid. The software used to analyze z-scan FCS data was generously provided by Dr. Jonas Ries.

References

1. Bromley, S. K.; Burack, W. R.; Johnson, K. G.; Somersalo, K.; Sims, T. N.; Sumen, C.; Davis, M. M.; Shaw, A. S.; Allen, P. M.; Dustin, M. L. The Immunological Synapse. *Annual Review of Immunology* **2001,***19* (1), 375-396.
2. Manz, B. N.; Groves, J. T. Spatial organization and signal transduction at intercellular junctions. *Nat Rev Mol Cell Biol* **2010,***11* (5), 342-52.
3. Hsu, C.-J.; Hsieh, W.-T.; Waldman, A.; Clarke, F.; Huseby, E. S.; Burkhardt, J. K.; Baumgart, T. Ligand Mobility Modulates Immunological Synapse Formation and T Cell Activation. *PLoS ONE* **2012,***7* (2), e32398.
4. Bunnell, S. C.; Hong, D. I.; Kardon, J. R.; Yamazaki, T.; McGlade, C. J.; Barr, V. A.; Samelson, L. E. T cell receptor ligation induces the formation of dynamically regulated signaling assemblies. *J Cell Biol* **2002,***158* (7), 1263-75.
5. Campi, G.; Varma, R.; Dustin, M. L. Actin and agonist MHC-peptide complex-dependent T cell receptor microclusters as scaffolds for signaling. *The Journal of experimental medicine* **2005,***202* (8), 1031-6.
6. Vogel, V.; Sheetz, M. Local force and geometry sensing regulate cell functions. *Nat. Rev. Mol. Cell Biol.* **2006,***7* (4), 265-275.
7. Dykstra, M.; Cherukuri, A.; Sohn, H. W.; Tzeng, S.-J.; Pierce, S. K. LOCATION IS EVERYTHING: Lipid Rafts and Immune Cell Signaling*. *Annual Review of Immunology* **2003,***21* (1), 457-481.
8. Chen, C. S.; Mrksich, M.; Huang, S.; Whitesides, G. M.; Ingber, D. E. Geometric Control of Cell Life and Death. *Science* **1997,***276* (5317), 1425-1428.
9. Fleire, S. J.; Goldman, J. P.; Carrasco, Y. R.; Weber, M.; Bray, D.; Batista, F. D. B Cell Ligand Discrimination Through a Spreading and Contraction Response. *Science* **2006,***312* (5774), 738-741.
10. Chan, P. Y.; Lawrence, M. B.; Dustin, M. L.; Ferguson, L. M.; Golan, D. E.; Springer, T. A. Influence of receptor lateral mobility on adhesion strengthening between membranes containing LFA-3 and CD2. *J Cell Biol* **1991,***115* (1), 245-255.
11. Batista, F. D.; Iber, D.; Neuberger, M. S. B cells acquire antigen from target cells after synapse formation. *Nature* **2001,***411* (6836), 489-94.
12. Ketchum, C.; Miller, H.; Song, W.; Upadhyaya, A. Ligand mobility regulates B cell receptor clustering and signaling activation. *Biophys J* **2014,***106* (1), 26-36.
13. Groves, J. T.; Dustin, M. L. Supported planar bilayers in studies on immune cell adhesion and communication. *J. Immunol. Methods* **2003,***278* (1-2), 19-32.
14. Weghuber, J.; Sunzenauer, S.; Plochberger, B.; Brameshuber, M.; Haselgrübler, T.; Schütz, G. J. Temporal resolution of protein–protein interactions in the live-cell plasma membrane. *Anal Bioanal Chem* **2010,***397* (8), 3339-3347.
15. Chiantia, S.; Ries, J.; Chwastek, G.; Carrer, D.; Li, Z.; Bittman, R.; Schwille, P. Role of ceramide in membrane protein organization investigated by combined AFM and FCS. *Biochimica et Biophysica Acta (BBA) - Biomembranes* **2008,***1778* (5), 1356-1364.
16. Ries, J.; Chiantia, S.; Schwille, P. Accurate Determination of Membrane Dynamics with Line-Scan FCS. *Biophysical Journal* **2009,***96* (5), 1999-2008.
17. Forstner, M. B.; Yee, C. K.; Parikh, A. N.; Groves, J. T. Lipid Lateral Mobility and Membrane Phase Structure Modulation by Protein Binding. *Journal of the American Chemical Society* **2006,***128* (47), 15221-15227.

18. Dustin, M. L.; Long, E. O. Cytotoxic immunological synapses. *Immunological Reviews* **2010,***235* (1), 24-34.
19. Lee, K.-H.; Feig, C.; Tchikov, V.; Schickel, R.; Hallas, C.; Schütze, S.; Peter, M. E.; Chan, A. C. The role of receptor internalization in CD95 signaling. *The EMBO Journal* **2006,***25* (5), 1009-1023.
20. Quist, A. P.; Pavlovic, E.; Oscarsson, S. Recent advances in microcontact printing. *Anal Bioanal Chem* **2005,***381* (3), 591-600.
21. Torres, A. J.; Wu, M.; Holowka, D.; Baird, B. Nanobiotechnology and Cell Biology: Micro- and Nanofabricated Surfaces to Investigate Receptor-Mediated Signaling. *Annual Review of Biophysics* **2008,***37* (1), 265-288.
22. Groves, J. T.; Boxer, S. G. Micropattern Formation in Supported Lipid Membranes. *Accounts of Chemical Research* **2002,***35* (3), 149-157.
23. Dontha, N.; Nowall, W. B.; Kuhr, W. G. Generation of biotin/avidin/enzyme nanostructures with maskless photolithography. *Anal. Chem.* **1997,***69* (14), 2619-2625.
24. James, C. D.; Davis, R. C.; Kam, L.; Craighead, H. G.; Isaacson, M.; Turner, J. N.; Shain, W. Patterned protein layers on solid substrates by thin stamp microcontact printing. *Langmuir* **1998,***14* (4), 741-744.
25. Kung, L. A.; Kam, L.; Hovis, J. S.; Boxer, S. G. Patterning Hybrid Surfaces of Proteins and Supported Lipid Bilayers. *Langmuir* **2000,***16* (17), 6773-6776.
26. Torres, A. J.; Vasudevan, L.; Holowka, D.; Baird, B. A. Focal adhesion proteins connect IgE receptors to the cytoskeleton as revealed by micropatterned ligand arrays. *Proceedings of the National Academy of Sciences* **2008,***105* (45), 17238-17244.
27. Offenhäusser, A.; Böcker-Meffert, S.; Decker, T.; Helpenstein, R.; Gasteier, P.; Groll, J.; Möller, M.; Reska, A.; Schäfer, S.; Schulte, P.; Vogt-Eisele, A. Microcontact printing of proteins for neuronal cell guidance. *Soft Matter* **2007,***3* (3), 290-298.
28. Roth, S.; Bugnicourt, G.; Bisbal, M.; Gory-Fauré, S.; Brocard, J.; Villard, C. Neuronal architectures with axo-dendritic polarity above silicon nanowires. *Small* **2012,***8* (5), 671-675.
29. Morigaki, K.; Mizutani, K.; Saito, M.; Okazaki, T.; Nakajima, Y.; Tatsu, Y.; Imaishi, H. Surface functionalization of a polymeric lipid bilayer for coupling a model biological membrane with molecules, cells, and microstructures. *Langmuir* **2013,***29* (8), 2722-30.
30. Yamada, M.; Imaishi, H.; Morigaki, K. Microarrays of phospholipid bilayers generated by inkjet printing. *Langmuir* **2013,***29* (21), 6404-8.
31. Wu, M.; Holowka, D.; Craighead, H. G.; Baird, B. Visualization of plasma membrane compartmentalization with patterned lipid bilayers. *Proceedings of the National Academy of Sciences of the United States of America* **2004,***101* (38), 13798-803.
32. Wu, M.; Baumgart, T.; Hammond, S.; Holowka, D.; Baird, B. Differential targeting of secretory lysosomes and recycling endosomes in mast cells revealed by patterned antigen arrays. *Journal of cell science* **2007,***120* (Pt 17), 3147-54.
33. Orth, R. N.; Wu, M.; Holowka, D. A.; Craighead, H. G.; Baird, B. A. Mast cell activation on patterned lipid bilayers of subcellular dimensions. *Langmuir* **2003,***19* (5), 1599-1605.
34. Kam, L.; Boxer, S. G. Cell adhesion to protein-micropatterned-supported lipid bilayer membranes. *Journal of biomedical materials research* **2001,***55* (4), 487-95.
35. Kunik, D.; Aramendia, P. F.; Martínez, O. E. Single photon fluorescent microlithography for live-cell imaging. *Microscopy Research and Technique* **2009**, NA-NA.
36. Truskett, V. N.; Watts, M. P. C. Trends in imprint lithography for biological applications. *Trends Biotechnol.* **2006,***24* (7), 312-317.

37. Tabeling, P. *Introduction to microfluidics*; Oxford University Press: Oxford, U.K. ; New York, 2005. p vii, 301p.
38. Costantino, S.; Heinze, K. G.; Martinez, O. E.; De Koninck, P.; Wiseman, P. W. Two-photon fluorescent microlithography for live-cell imaging. *Microsc Res Tech* **2005,***68* (5), 272-6.
39. Nagata, S. Apoptosis by death factor. *Cell* **1997,***88* (3), 355-65.
40. Peter, M. E.; Krammer, P. H. The CD95(APO-1/Fas) DISC and beyond. *Cell death and differentiation* **2003,***10* (1), 26-35.
41. Day, C. A.; Kraft, L. J.; Kang, M.; Kenworthy, A. K. Analysis of protein and lipid dynamics using confocal fluorescence recovery after photobleaching (FRAP). *Curr Protoc Cytom* **2012,***Chapter 2*, Unit2.19.
42. Axelrod, D.; Koppel, D. E.; Schlessinger, J.; Elson, E.; Webb, W. W. Mobility measurement by analysis of fluorescence photobleaching recovery kinetics. *Biophys J* **1976,***16* (9), 1055-69.
43. Soumpasis, D. M. Theoretical analysis of fluorescence photobleaching recovery experiments. *Biophys J* **1983,***41* (1), 95-7.
44. García-Sáez, A. J.; Carrer, D. C.; Schwille, P. Fluorescence Correlation Spectroscopy for the Study of Membrane Dynamics and Organization in Giant Unilamellar Vesicles. In *Liposomes*, Weissig, V., Ed.; Humana Press: Totowa, NJ, 2010; Vol. 606, pp 493-508.
45. Macháň, R.; Hof, M. Lipid diffusion in planar membranes investigated by fluorescence correlation spectroscopy. *Biochimica et Biophysica Acta (BBA) - Biomembranes* **2010,***1798* (7), 1377-1391.
46. Benda, A.; Beneš, M.; Marecek, V.; Lhotskỳ, A.; Hermens, W. T.; Hof, M. How to determine diffusion coefficients in planar phospholipid systems by confocal fluorescence correlation spectroscopy. *Langmuir* **2003,***19* (10), 4120-4126.
47. Yu, C.-h.; Groves, J. T. Engineering supported membranes for cell biology. *Med Biol Eng Comput* **2010,***48* (10), 955-963.
48. LA, O. R.; Tai, L.; Lee, L.; Kruse, E. A.; Grabow, S.; Fairlie, W. D.; Haynes, N. M.; Tarlinton, D. M.; Zhang, J. G.; Belz, G. T.; Smyth, M. J.; Bouillet, P.; Robb, L.; Strasser, A. Membrane-bound Fas ligand only is essential for Fas-induced apoptosis. *Nature* **2009,***461* (7264), 659-63.
49. Weiss, J. M.; Subleski, J. J.; Back, T.; Chen, X.; Watkins, S. K.; Yagita, H.; Sayers, T. J.; Murphy, W. J.; Wiltrout, R. H. Regulatory T cells and myeloid-derived suppressor cells in the tumor microenvironment undergo Fas-dependent cell death during IL-2/alphaCD40 therapy. *Journal of immunology* **2014,***192* (12), 5821-9.
50. Steinberger, T.; Machan, R.; Hof, M. Z-scan fluorescence correlation spectroscopy as a tool for diffusion measurements in planar lipid membranes. *Methods in molecular biology* **2014,***1076*, 617-34.
51. Sterling, S. M.; Allgeyer, E. S.; Fick, J.; Prudovsky, I.; Mason, M. D.; Neivandt, D. J. Phospholipid diffusion coefficients of cushioned model membranes determined via z-scan fluorescence correlation spectroscopy. *Langmuir* **2013,***29* (25), 7966-74.
52. Hovis, J. S.; Boxer, S. G. Patterning and Composition Arrays of Supported Lipid Bilayers by Microcontact Printing. *Langmuir* **2001,***17* (11), 3400-3405.
53. Kahya, N.; Schwille, P. How phospholipid-cholesterol interactions modulate lipid lateral diffusion, as revealed by fluorescence correlation spectroscopy. *Journal of fluorescence* **2006,***16* (5), 671-8.

54. Przybylo, M.; Sykora, J.; Humpolickova, J.; Benda, A.; Zan, A.; Hof, M. Lipid diffusion in giant unilamellar vesicles is more than 2 times faster than in supported phospholipid bilayers under identical conditions. *Langmuir* **2006,***22* (22), 9096-9.
55. Batista, F. D.; Dustin, M. L. Cell:cell interactions in the immune system. *Immunol Rev* **2013,***251* (1), 7-12.
56. Peter, H. H.; Warnatz, K. Molecules involved in T-B co-stimulation and B cell homeostasis: possible targets for an immunological intervention in autoimmunity. *Expert opinion on biological therapy* **2005,***5 Suppl 1*, S61-71.
57. Krzewski, K.; Bryceson, Y. T. Molecular mechanisms regulating cytotoxic lymphocyte development and function, and their associations to human diseases. *Frontiers in immunology* **2014,***5*, 279.
58. Davis, D. M.; Dustin, M. L. What is the importance of the immunological synapse? *Trends in immunology* **2004,***25* (6), 323-7.
59. Falconnet, D.; Csucs, G.; Grandin, H. M.; Textor, M. Surface engineering approaches to micropattern surfaces for cell-based assays. *Biomaterials* **2006,***27* (16), 3044-63.
60. Mossman, K.; Groves, J. Micropatterned supported membranes as tools for quantitative studies of the immunological synapse. *Chemical Society reviews* **2007,***36* (1), 46-54.
61. Milone, M. C.; Kam, L. C. Investigative and clinical applications of synthetic immune synapses. *Wiley Interdisciplinary Reviews: Nanomedicine and Nanobiotechnology* **2013,***5* (1), 75-85.
62. June, C. H. Principles of adoptive T cell cancer therapy. *The Journal of clinical investigation* **2007,***117* (5), 1204-12.
63. Dale, B. M.; Alvarez, R. A.; Chen, B. K. Mechanisms of enhanced HIV spread through T-cell virological synapses. *Immunol Rev* **2013,***251* (1), 113-24.
64. Batista, F. D.; Neuberger, M. S. B cells extract and present immobilized antigen: implications for affinity discrimination. *EMBO J* **2000,***19* (4), 513-20.
65. Hammond, S.; Wagenknecht-Wiesner, A.; Veatch, S. L.; Holowka, D.; Baird, B. Roles for SH2 and SH3 domains in Lyn kinase association with activated FcepsilonRI in RBL mast cells revealed by patterned surface analysis. *J Struct Biol* **2009,***168* (1), 161-7.
66. Dustin, M. L. Supported bilayers at the vanguard of immune cell activation studies. *Journal of Structural Biology* **2009,***168* (1), 152-160.
67. Hsu, C. J.; Hsieh, W. T.; Waldman, A.; Clarke, F.; Huseby, E. S.; Burkhardt, J. K.; Baumgart, T. Ligand mobility modulates immunological synapse formation and T cell activation. *PLoS One* **2012,***7* (2), e32398.
68. Vieu, C.; Carcenac, F.; Pepin, A.; Chen, Y.; Mejias, M.; Lebib, A.; Manin-Ferlazzo, L.; Couraud, L.; Launois, H. Electron beam lithography: resolution limits and applications. *Applied Surface Science* **2000,***164* (1), 111-117.
69. Castellana, E. T.; Cremer, P. S. Solid supported lipid bilayers: From biophysical studies to sensor design. *Surface Science Reports* **2006,***61* (10), 429-444.
70. Bally, M.; Bailey, K.; Sugihara, K.; Grieshaber, D.; Vörös, J.; Städler, B. Liposome and Lipid Bilayer Arrays Towards Biosensing Applications. *Small* **2010,***6* (22), 2481-2497.
71. Mujahid, A.; Iqbal, N.; Afzal, A. Bioimprinting strategies: from soft lithography to biomimetic sensors and beyond. *Biotechnology advances* **2013,***31* (8), 1435-47.

TOC Graphic